Bioconjugate Chemistry

Article

pubs.acs.org/bc

Excimer Emission Properties on Pyrene-Labeled Protein Surface: Correlation between Emission Spectra, Ring Stacking Modes, and Flexibilities of Pyrene Probes

Akira Fujii,[†] Yutaka Sekiguchi,[†] Hiroyoshi Matsumura,*[,‡] Tsuyoshi Inoue,[‡] Wen-Sheng Chung,*[,§] Shun Hirota,[†] and Takashi Matsuo*[,†]

[†]Graduate School of Materials Science, Nara Institute of Science and Technology (NAIST), Ikoma, Nara 630-0192, Japan

[‡]Department of Applied Chemistry, Graduate School of Engineering, Osaka University, 2-1 Yamadaoka, Suita, Osaka 565-0871, Japan

[§]Department of Applied Chemistry, National Chiao Tung University, Hsinchu, 30050, Taiwan, Republic of China

Supporting Information

ABSTRACT: The excimer emission of pyrene is popularly employed for investigating the association between pyrene-labeled biomolecules or between pyrene-labeled places in a biomolecule. The property of pyrene excimer emission is affected by the fluctuation in ring stacking modes, which originates from the structural flexibilities of pyrene probes and/or of labeled places. Investigations of the excimer emission in terms of dynamics of pyrene stacking modes provide the detailed spatial information between pyrene-labeled places. In order to evaluate the effects of probe structures and fluctuation in pyrene−pyrene association modes on their emission properties on protein surface, three types of pyrene probe with different linker lengths were synthesized and conjugated to two cysteine residues in the A55C/C77S/V169C mutant of adenylate kinase (Adk), an enzyme that shows a structural transition between OPEN and CLOSED forms. In the CLOSED form of Adk labeled by a pyrene probe with a short linker, excimer emission was found to be predominated by the ground-state association of pyrenes. The pyrene stacking structure on the protein surface was successfully determined by an X-ray crystallographic analysis. However, the emission decay in the protein suggested the existence of several stacking orientations in solution. With the increase in the linker length, the effect of fluctuation in pyrene association modes on the spectral properties distinctly emerged at both ground and excited states. The combination of steady-state and time-resolved spectroscopic analyses is useful for differentiation in the origin of the excimer emission, which is essential for precisely understanding the interaction fashions between pyrene-labeled biomolecules.

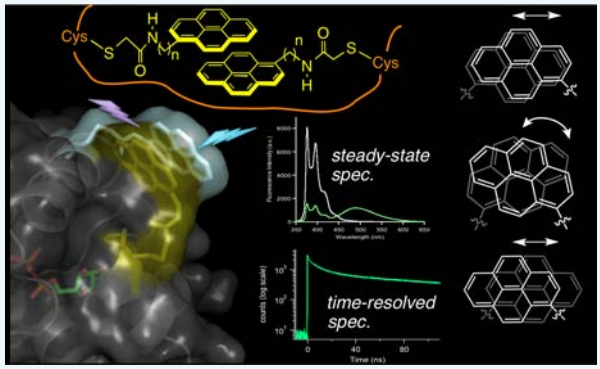

INTRODUCTION

Pyrene is a typical bioprobe for evaluating the interactions between various biomolecules, because its emission property distinctly depends on the distance between two pyrene rings. Since the change in the emission spectrum is readily detectable by conventional fluorescence measurements under dilute conditions, various pyrene-labeled biomolecules (e.g., proteins/peptides,[1,2] DNA/RNA,[3−5] fatty acids,[6,7] phospholipids,[8,9] etc.) have been developed. An isolated pyrene has an emission band in the range of 380−400 nm on excitation around 340 nm ("monomer emission"), whereas the proximity of two pyrenes produces a new emission band in a longer wavelength range ("excimer emission").[10−12] The spectral change in the fluorescence of pyrene is also useful for obtaining the spatial information between two places in a single protein molecule without considering protein−protein interactions.[13,14] Furthermore, substituted pyrene derivatives with high quantum yields in water[15] and a variety of pyrene-based metal ion sensors[16,17] have been reported.

In most of biochemical works using pyrene probes, the intensity of excimer emission obtained by steady-state fluorescence measurements is mainly used for evaluating the proximity of pyrene-labeled biomolecules. However, the excimer emission of pyrene is, in fact, classified into two types based on the association mode of two pyrene rings.[18] One is the emission derived from a dimer formed in the excited state but rather dissociative in the ground state ("dynamic excimer").[19] The other is the emission of a preassociated pyrene complex in the ground state ("static excimer"). Because both the types of emission appear as a broad spectral band at a very similar wavelength region, their differentiation between the two mechanisms of excimer emission is difficult in conventional steady-state fluorescence measurements. However, the effect of pyrene association modes on the excimer emission property

Received: January 13, 2015
Revised: February 2, 2015
Published: February 3, 2015

DOI: 10.1021/acs.bioconjchem.5b00026
Bioconjugate Chem. 2015, 26, 537−548

becomes critical, when the flexibility of a probe molecule and/or probe-labeled places in a biomolecule increase. Nevertheless, the excimer emission mechanism from the viewpoint of structural dynamics in a pyrene dimer is rarely discussed in biochemical analyses using pyrene probes, although the effect of the fluctuation in pyrene−pyrene stacking on the emission properties has often been discussed in pyrene-pendant synthetic polymers.[20−25] The quantitative analysis of this subject is essential for optimizing the structure of pyrene probes to correctly detect the association mode between pyrene-labeled biomolecules or between pyrene-labeled places in a biomolecule.

Previously, we demonstrated a switching in the fluorescence property of pyrene using the protein motion of adenylate kinase (Adk),[26] a Mg^{2+}-dependent enzyme catalyzing the phosphoryl transfer between ATP, ADP, and AMP.[27,28] The enzyme has two subdomains, NMP and LID domains (see the structure in Figure 1, left), and binds ADP to each domain, producing AMP and Mg^{2+}·ATP at the former and latter domains, respectively. In the reversed reaction, AMP and Mg^{2+}·ATP selectively bind to their respective domains.[29] The substrate-binding/product release is accompanied by a reversible domain-based structural transition ("OPEN form" and "CLOSED form" in Figure 1).[29,30] During the conformational change, the distance between Ala55 and Val169 changes by ca. 20 Å.[29,30] Considering these structural features, we have mutated these amino acid residues into cysteine to prepare a triple mutant of Adk (namely, Adk_{tm} ; where "tm" means triple mutant: Ala55Cys, Val169Cys, and Cys77Ser). By conjugating pyrene to the thiol groups at Cys55 and Cys169, we aimed at a reversible change in the distance between the pyrenes. Upon the addition of ADP or Ap_5A (P^1,P^5-diadenosine 5′-pentaphosphate, a transition state analog for Adk) to the pyrene-labeled Adk_{tm}, the protein showed characteristic excimer emission around 485 nm with the decrease in its monomer emission. The spectral change is observable under dilute conditions (less than 10^{-6} M), indicative of a phenomenon caused by the motion of a single protein molecule (without interprotein process).

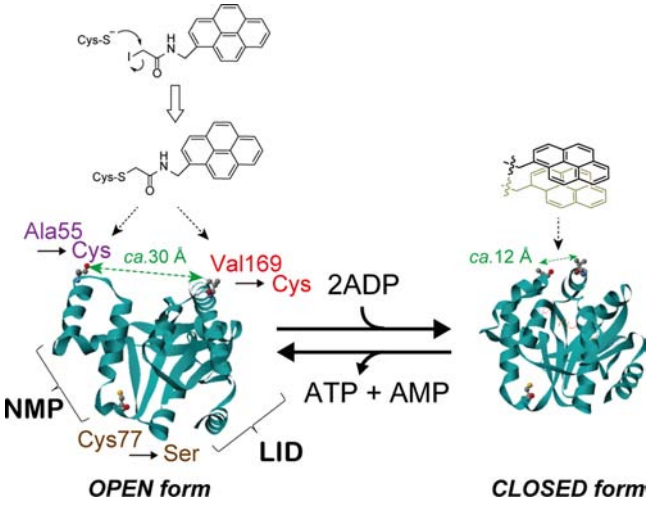

Figure 1. Reversible switching system for pyrene emission property driven by motion of Adk_{tm}. The OPEN and CLOSED forms of Adk are based on the structures of PDB ID 1AKE and 4AKE, respectively. "NMP" and "LID" stand for the domains producing AMP and Mg^{2+}·ATP from two molecules of ADP. In reverse reaction, these nucleotides bind to the corresponding domains.

In the CLOSED Adk_{tm}, cysteine-mutated positions are on rigid α-helix backbones. Hence, the pyrene-labeled Adk_{tm} is a suitable scaffold for straightforward study of the correlation between the origin of excimer emission and the flexibility of a pyrene probe. Accordingly, we prepared **C1**-, **C2**-, and **C3**-Adk_{tm}s, where the two cysteine residues of Adk_{tm}s were modified by three kinds of alkyl pyrene with varying lengths of methylene linkers (**C1**, **C2**, and **C3**, respectively; see the structures in Figure 2). Subsequently, the emission properties of these modified proteins were investigated using steady-state and time-resolved fluorescence spectroscopies. **C1**-Adk_{tm} is the same modified enzyme as reported previously.[26] In these proteins, a common scaffold biomolecule (Adk_{tm}) with fixed sites for conjugation (Cys55 and Cys169) allows us to selectively extract the effect of structural flexibility of the linker moiety on the ring stacking modes of pyrenes at the protein surface. As a result, it was found that the excimer emission intensity in the CLOSED forms of Adk_{tm}s is highly dependent on the linker length in spite of similar distance between the two pyrene-labeled cysteine residues. Time-resolved fluorescence analysis on the decay of the excimer emission for the protein indicated that several stacking modes exist in solutions. The spectroscopic results highlight the utility of the combination of steady-state and time-resolved spectroscopic measurements for the quantitative analysis of interactions between labeled acid residues in a protein considering the structural flexibilities of probe molecules.

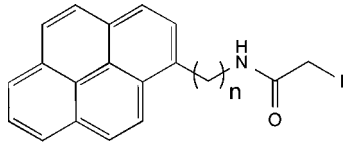

n = 1 : **C1**
n = 2 : **C2**
n = 3 : **C3**

Figure 2. Structures of pyrenyl iodoacetamides **C1**, **C2**, and **C3**.

RESULTS

Syntheses of Pyrenyl Iodoacetamide Compounds. Pyrenyl iodoacetamides **C2** and **C3** were synthesized from readily available pyrene derivatives (Scheme 1). 1-Pyrenecarbaldehyde (**1**) was converted into ethyl pyrenyl acrylate **2** by a Horner-Wadsworth-Emmons-type reaction in the presence of LiCl.[31] The olefin moiety in **2** was reduced by $NaBH_4$ in the presence of $CoCl_2$, followed by saponification to yield pyreneylpropionic acid **4**. The carboxylic acid moiety in **4** was then converted into a benzyloxycarbonyl-protected amino group via Curtius rearrangement using diphenylphosphoryl azide (DPPA). After the deprotection of the benzyloxycarbonyl group by HBr, the resultant free amine was reacted with the hydroxysuccinimide ester of iodoacetic acid (HSIA) to yield **C2**. Compound **C3** was derived from (1-pyrenyl)butyric acid (**7**), a commercially available pyrene, by the same synthetic route as that starting from **4**.

Secondary Structures and Enzymatic Activities of Pyrene-Labeled Adk_{tm}s. The CD spectra in UV region for Adk_{tm}s (Supporting Information Figure S1) showed no

DOI: 10.1021/acs.bioconjchem.5b00026
Bioconjugate Chem. 2015, 26, 537−548

Scheme 1. Syntheses of Pyrenyl Iodoacetamides C2 and C3

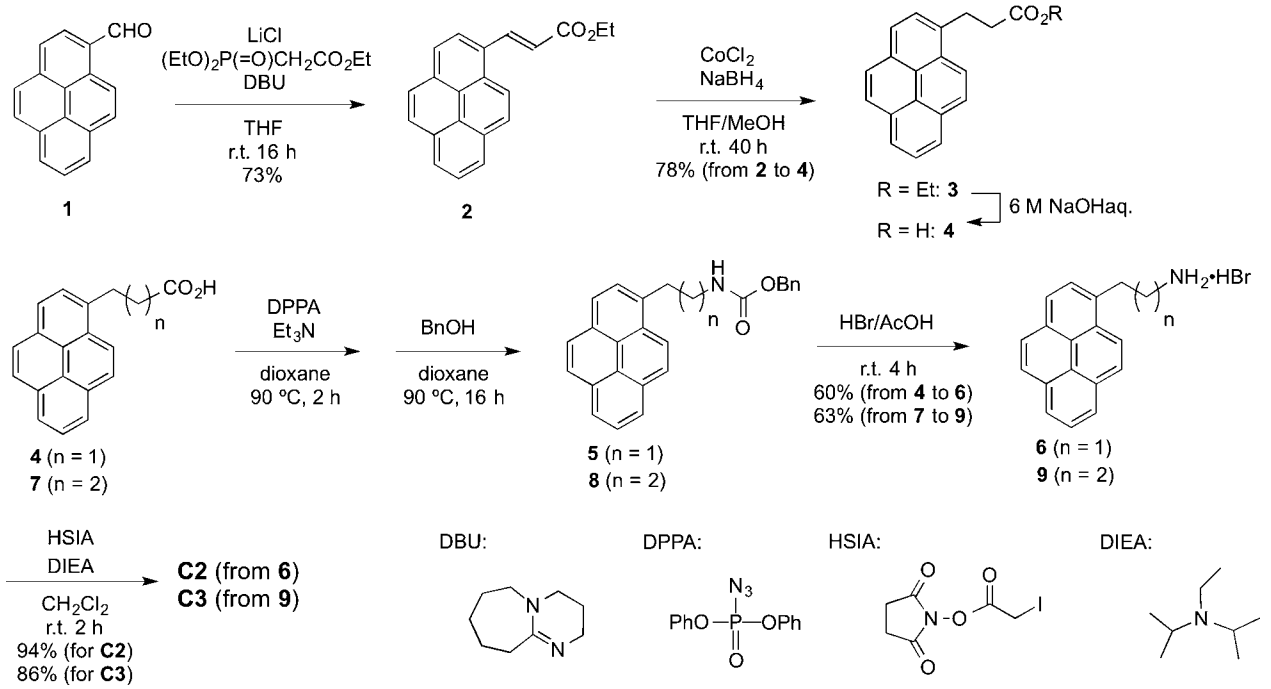

significant denaturation after the chemical modification of Adk_{tm}. The phosphoryl transfer activities of the pyrene-labeled Adk_{tm}s were confirmed by colorimetric measurements using a coupled reaction with the hexokinase/glucose-6-phosphate dehydrogenase tandem catalysis system (see Scheme S1 and Figure S2 in Supporting Information).[32] All the pyrene-labeled Adk_{tm}s showed the production of NADPH (a product resulted from the final step of the tandem reaction; the increase in absorbance at 340 nm). These findings indicate that the chemical modification of the protein surface exerted no significant influence on the active site structure. The catalytic activities of the pyrene-labeled Adk_{tm}s were, however, smaller than that of the unmodified Adk_{tm} by 20−35% (based on the amount of produced NADPH at 40 s). The reduction in the overall catalytic activity may be attributed to the partial inhibition of product release from the Adk_{tm} matrix by the pyrene rings on the protein surface.

Steady-State Fluorescence Spectra of Pyrene-Labeled Adk_{tm}s with Nucleotide Ligands. The phosphoryl transfer activities observed in the pyrene-labeled Adk_{tm}s indicate that all the proteins adopt a corresponding CLOSED form on the substrate binding. Thus, we can expect that the two pyrene rings are in proximity with the protein surface on the nucleotide substrate binding. At first, we measured fluorescence spectral changes on the addition of Ap_5A (P^1,P^5-diadenosine 5′-pentaphosphate), a transition state analog for Adk, to a protein solution. We also investigated the effect of Mg^{2+} on the spectral changes, since Mg^{2+} is a cofactor for the phosphoryl transfer activity of Adk. The observed fluorescence spectral changes are presented in Figure 3. The ratios of emission intensities between the monomer and excimer emissions ($I_R = I_E/I_M$, where I_E is the emission intensity at 485 nm and I_M is the emission intensity at 376 nm (for **C1**-Adk_{tm}) or 377 nm (for **C2**- and **C3**-Adk_{tm}s)) are listed in Table 1. The overall fluorescence quantum yields (Φ_Fs, expressed as a value for two pyrene moieties) are also included in Table 1.

As previously reported, data for **C1**-Adk_{tm},[26] **C2**- and **C3**-Adk_{tm}s also displayed a decrease in the emission intensity around 380 nm (monomer emission) upon the addition of Ap_5A, whereas a new broad emission band (excimer emission) appeared around 485 nm (Figure 3b,c).[33] This result allows us to discuss the effect of the methylene linker on the pyrene emission properties present on the protein surface. In the presence of Ap_5A, the emission intensity of these Adk_{tm}s around 485 nm is ranked as **C1**-Adk_{tm} > **C2**-Adk_{tm} > **C3**-Adk_{tm} (Figure 3d). The value of I_R (I_E/I_M ratio) also showed a similar trend. **C1**-Adk_{tm} showed a further increase in the emission intensity at 485 nm in the presence of Mg^{2+} (the blue line in Figure 3a). This is associated with the change in the pyrene−pyrene interaction mode caused by the formation of an Ap_5A-Mg^{2+}-enzyme ternary complex (vide infra).[34] In contrast, little effect of Mg^{2+} was observed in the emission intensities at 485 nm and I_R values of **C2**- and **C3**-Adk_{tm}s.

The fluorescence spectral changes were also observed after the addition of ADP, ATP, or AMP (Figure S3 in Supporting Information). In the spectral changes of **C2**- and **C3**-Adk_{tm}s, the intensity of the excimer emission at 485 nm is ranked +ADP > +ATP > +AMP. This trend is also the same as that previously observed in **C1**-Adk_{tm}.[26]

The fluorescence quantum yields of the pyrene-labeled Adk_{tm}s determined under N_2 atmosphere or air were similar, indicating that the emissions were all from the singlet excited states. **C3**-Adk_{tm} was found to have the smallest Φ_F among the three modified Adk_{tm}s regardless of the presence or the absence of Ap_5A. The Φ_F values of the Adk_{tm} in the presence of Ap_5A (i.e., in CLOSED forms) decreased from those in the absence of it (i.e., in OPEN forms); especially, **C2**-Adk_{tm} showed the highest decrease in Φ_F value.

UV−vis and Excitation Spectra of Pyrene-Labeled Adk_{tm}s. All the pyrene-labeled Adk_{tm}s showed absorption bands in the range from 300 to 370 nm. The CLOSED **C1**-Adk_{tm} showed a broadened spectrum, compared to that of the corresponding OPEN-form protein (Figure 4a). The spectral

DOI: 10.1021/acs.bioconjchem.5b00026
Bioconjugate Chem. 2015, 26, 537−548

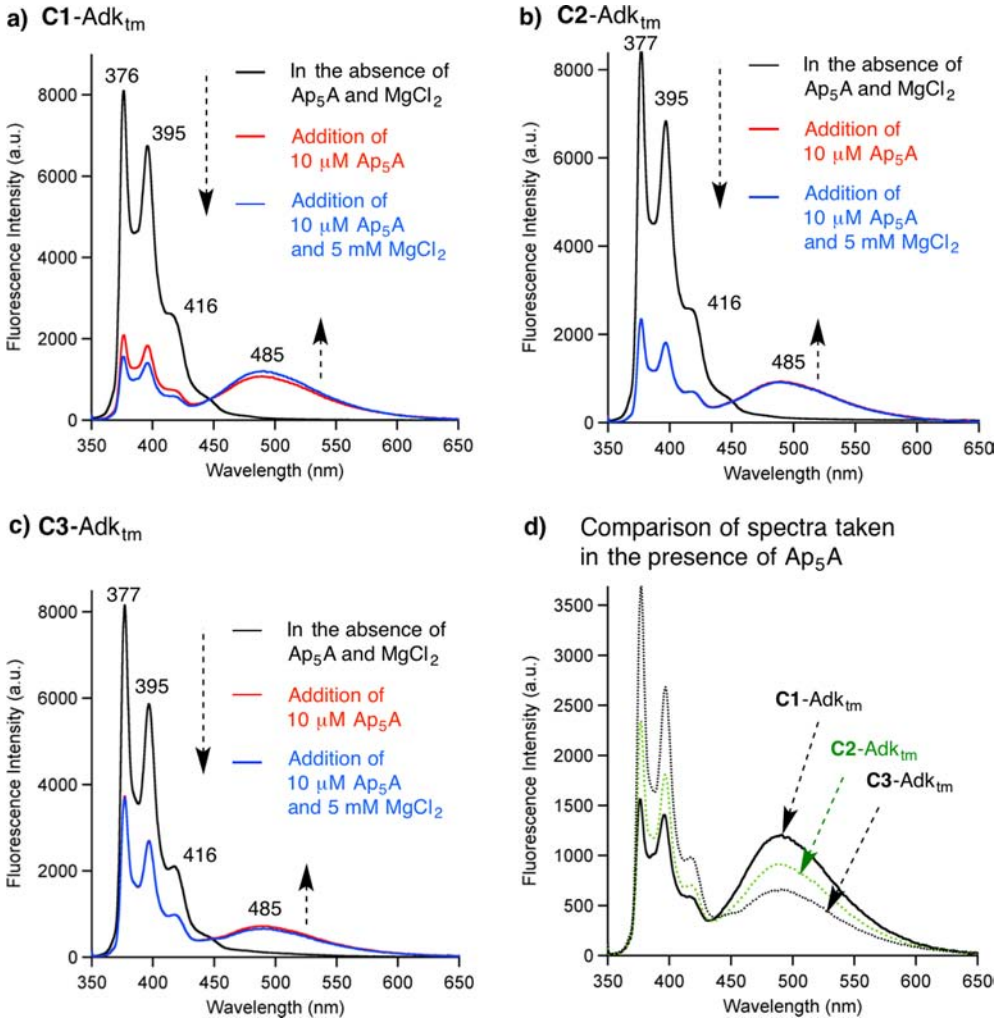

Figure 3. Steady-state fluorescence spectral change (λ_{ex} = 345 nm) for pyrene-labeled Adk$_{tm}$s on the addition of Ap$_5$A and MgCl$_2$ to Adk$_{tm}$ in 50 mM Tris buffer (pH = 7.5) at 25 °C under a N_2 atmosphere: (a) **C1**-Adk$_{tm}$; (b) **C2**-Adk$_{tm}$; (c) **C3**-Adk$_{tm}$. (d) Collected spectra taken in the presence of Ap$_5$A and MgCl$_2$. Final concentrations: [protein] = 0.18 μM, [Ap$_5$A] = 10 μM, and [MgCl$_2$] = 5 mM. The black, red, and blue spectra were obtained in the absence of Ap$_5$A and MgCl$_2$, in the presence of only Ap$_5$A, and in the presence of both Ap$_5$A and MgCl$_2$, respectively. In (d), the solid black, dotted green, and dotted black lines indicate the spectra in the presence of Ap$_5$A for **C1**-Adk$_{tm}$, **C2**-Adk$_{tm}$, and **C3**-Adk$_{tm}$, respectively.

Table 1. Ratio of Intensities between Excimer and Monomer Emissions (I_R) and Fluorescence Quantum Yield (Φ_F)[a]

Protein	**C1**-Adk$_{tm}$			**C2**-Adk$_{tm}$			**C3**-Adk$_{tm}$		
[Ap$_5$A]	no	10 μM	10 μM	no	10 μM	10 μM	no	10 μM	10 μM
[MgCl$_2$]	no	0 mM	5 mM	no	0 mM	5 mM	no	0 mM	5 mM
I_R[b]	0.006	0.50	0.95	0.010	0.41	0.41	0.030	0.18	0.19
$\Phi_{F(N2)}$[c]	0.37	0.25	0.24	0.37	0.21	0.21	0.31	0.23	0.22
$\Phi_{F(air)}$[d]	0.35	0.24	0.22	0.32	0.18	0.18	0.28	0.19	0.19

[a]50 mM Tris buffer (pH = 7.5) at 25 °C, λ_{ex} = 345 nm. [b]$I_R = I_E/I_M$, where I_E is emission intensity at 485 nm and I_M is emission intensity at 376 nm (for **C1**-Adk$_{tm}$) or 377 nm (for **C2**- and **C3**-Adk$_{tm}$s). [c]Fluorescence quantum yield (relative to 9,10-diphenylanthracene) under N_2. [d]Fluorescence quantum yield (relative to 9,10-diphenylanthracene) under air.

broadening in the CLOSED **C2**- and **C3**-Adk$_{tm}$s was smaller than that in **C1**-Adk$_{tm}$ (Figure 4b,c). The spectral broadening in the CLOSED proteins is related to a pyrene−pyrene association in the ground state (vide infra).[18]

The excitation spectra of the CLOSED-form proteins with the emissions at 375 or 485 nm are shown in Figure S4 in Supporting Information. The spectroscopic data are also useful for elucidating the mechanism of excimer emission.[18] As with the UV−vis spectra, the excitation spectra of the CLOSED **C1**-Adk$_{tm}$ showed a distinct spectral broadening when the emission wavelength was set at 485 nm. Here, the values of $P_{A(OPEN)}$, $P_{A(CLOSED)}$, P_M and P_E were calculated in order to correlate the spectral broadening with the pyrene−pyrene association mode quantitatively (Table 2). The values of $P_{A(OPEN)}$ and $P_{A(CLOSED)}$ are the peak-to-valley ratios in the UV−vis spectra for the OPEN-form and CLOSED-form proteins, respectively. The values of P_M and P_E stand for the peak-to-valley ratios in the excitation spectra of CLOSED proteins at monomer emission and excimer emission, respectively. The values of ΔP_{abs} (= $P_{A(OPEN)} - P_{A(CLOSED)}$) and ΔP_{excit} (= $P_M - P_E$) are the

DOI: 10.1021/acs.bioconjchem.5b00026
Bioconjugate Chem. 2015, 26, 537−548

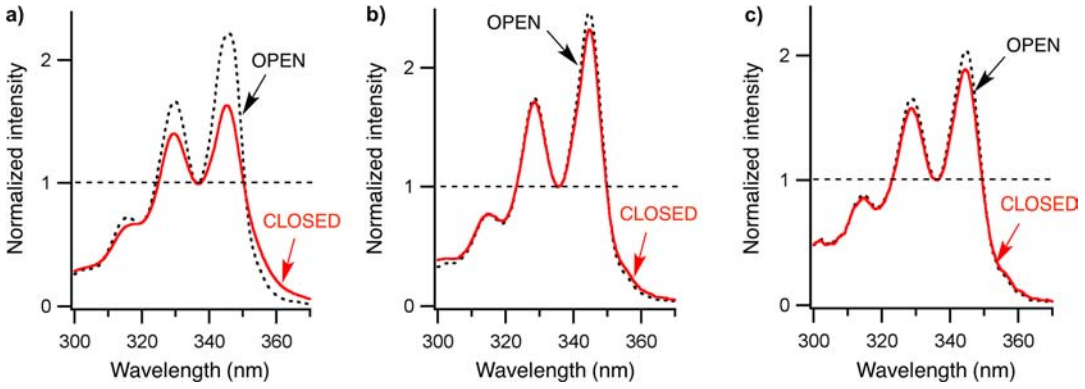

Figure 4. UV−vis spectra for OPEN/CLOSED pyrene-labeled Adk$_{tm}$s in 50 mM Tris buffer (pH = 7.5) at 25 °C: (a) **C1**-Adk$_{tm}$; (b) **C2**-Adk$_{tm}$; (c) **C3**-Adk$_{tm}$. All spectra are represented by a normalized absorbance based on the value at the spectral valley (336 nm). Black dotted lines and red solid lines indicate the spectra in the absence and presence of Ap$_5$A, respectively (i.e., OPEN and CLOSED forms), where [protein] = 0.18 μM, [Ap$_5$A] = 0 or 10 μM.

Table 2. Peak-to-Valley Ratios in UV−vis and Excitation Spectra of Pyrene-Labeled Adk$_{tm}$s[a]

	C1-Adk$_{tm}$	**C2**-Adk$_{tm}$	**C3**-Adk$_{tm}$
$P_{A(OPEN)}$[b]	2.22	2.46	2.04
$P_{A(CLOSED)}$[c]	1.61	2.32	1.88
ΔP_{abs}[d]	0.61	0.14	0.16
P_M[e]	2.46	2.74	2.36
P_E[f]	1.64	2.26	1.78
ΔP_{excit}[g]	0.82	0.48	0.58

[a] 50 mM Tris buffer, pH 7.5 at 25 °C, [protein] = 0.18 μM and [Ap$_5$A] = 0 μM (for proteins with OPEN form) or 10 μM (for proteins with CLOSED form). [b] $P_{A(OPEN)} = Abs_{346}/Abs_{336}$ in UV−vis spectra in OPEN-form proteins, where Abs_{346} and Abs_{336} are absorbances at 346 and 336 nm, respectively. [c] $P_{A(CLOSED)} = Abs_{346}/Abs_{336}$ in UV−vis spectra in CLOSED-form proteins. [d] $\Delta P_{abs} = P_{A(OPEN)} - P_{A(CLOSED)}$. [e] $P_M = I_{346}/I_{336}$ in excitation spectra at monomer emission (375 nm), where I_{346} and I_{336} are relative intensity at 346 and 336 nm, respectively. [f] $P_E = I_{346}/I_{336}$ in the excitation spectra at excimer emission (485 nm). [g] $\Delta P_{excit} = P_M - P_E$.

broadening factors for UV−vis and excitation spectra, respectively. In both the broadening factors, **C1**-Adk$_{tm}$ had larger values than those of the **C2**- and **C3**-Adk$_{tm}$. This indicates that the preassociation of pyrenes in the CLOSED **C1**-Adk$_{tm}$ in the ground state is most significant among Adk$_{tm}$s.

CD Spectra of Pyrene-Labeled Adk$_{tm}$s in CLOSED Form. The CD spectra of pyrene-labeled Adk$_{tm}$s in the ^1L_a absorption band region were collected for the characterization of pyrene−pyrene association in terms of its exciton coupling (Figure S5 in Supporting Information). According to our previous report,[26] the CLOSED **C1**-Adk$_{tm}$ shows a negative Cotton effect at the ^1L_a absorption band, whereas the OPEN **C1**-Adk$_{tm}$ shows no typical exciton coupling-type signal (Supporting Information Figure S5b). In contrast, the CLOSED **C2**-Adk$_{tm}$ showed no distinct CD signal in the ^1L_a absorption band region (Supporting Information Figure S5c). Interestingly, **C2**-Adk$_{tm}$ displayed CD signals with small intensities and positive sign in the OPEN form. Although the CD signals also appeared in **C3**-Adk$_{tm}$ on the addition of Ap$_5$A (Supporting Information Figure S5d), the signal sign was also always positive over this region. The signals observed in **C2**- and **C3**-Adk$_{tm}$s are attributed to the "induced CD signals" caused by interactions between the pyrene rings and peptide backbones/side chains in the vicinity of pyrene rings,[35−37] and not by pyrene−pyrene interactions.

X-ray Crystal Structure of the CLOSED Form of C1-Adk$_{tm}$. The spectral characteristics for the CLOSED **C1**-Adk$_{tm}$ shown above prompted us to conduct an X-ray crystallographic analysis of the CLOSED **C1**-Adk$_{tm}$ in order to acquire detailed structural information on the pyrene−pyrene interactions present on the protein surface. Figure 5 displays the 2.8 Å resolution structure of the CLOSED **C1**-Adk$_{tm}$ in the presence of Ap$_5$A and a magnesium ion. Data collection statistics and

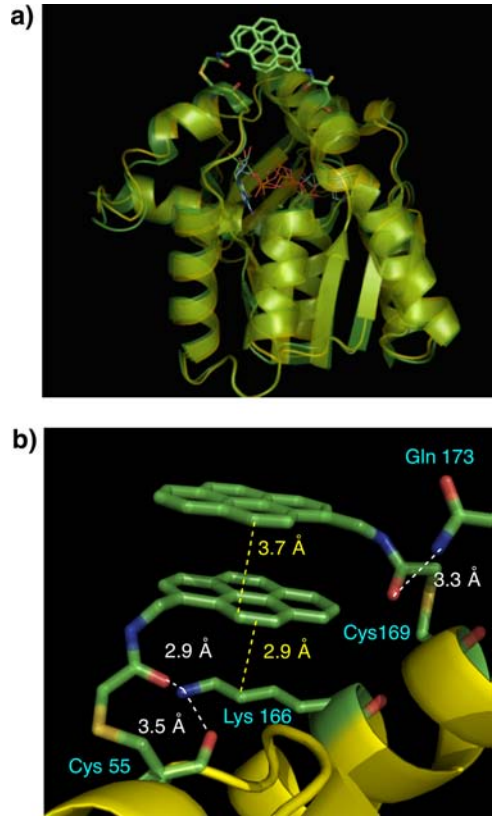

Figure 5. X-ray crystal structure of the CLOSED **C1**-Adk$_{tm}$ (2.8 Å resolution, PDB ID: 3X2S): (a) whole structure of CLOSED **C1**-Adk$_{tm}$ (yellow) superimposed with CLOSED wild-type Adk (PDB: 1AKE, green); (b) magnified figure in the vicinity of pyrene rings.

DOI: 10.1021/acs.bioconjchem.5b00026
Bioconjugate Chem. 2015, 26, 537−548

refinement statistics for both coordinate sets are summarized in Table S1 (Supporting Information). Superimposition of the structures for the CLOSED **C1**-Adk$_{tm}$ and the CLOSED wild-type Adk (PDB ID: 1AKE) (Figure 5a) indicated that the two structures are very similar; the root-mean-square (r.m.s.) deviation is 0.61 Å for 214 Cα pairs. In the CLOSED **C1**-Adk$_{tm}$, it was found that (i) the pyrene-labeled amino acid residues (Cys55 and Cys169) are located on α-helices; (ii) two pyrene ring moieties are protruding from the Adk$_{tm}$ matrix; (iii) they stack with a face-to-face orientation at a distance of 3.7 Å. The face-to-face orientation of two pyrene rings on the protein surface was assisted by several noncovalent interactions (Figure 5b): (i) the hydrogen bonding between Gln173 and the amide C═O group connecting a pyrene with Cys169 (N(−H)···O═C, 3.3 Å); (ii) the hydrogen bonding network composed of the backbone amide C═O group in Cys55, the side-chain amino group in Lys166, and the amide C═O group connecting a pyrene with Cys55 (C═O (backbone)−(H_3^+)N-Lys166 = 3.5 Å; Lys166 N(H_3^+)···O═C (amide connecting the pyrene) = 2.9 Å); (iii) C−H···π interaction between the pyrene ring and Lys166 side chain. In the crystal lattice, each paired pyrene ring is located more than 47 Å apart from the neighboring pyrene ring.

Fluorescence Lifetimes. In order to consider the pyrene emission properties from the viewpoint of the probe structures and the fluctuation in pyrene stacking modes, we conducted time-resolved fluorescence measurements using the time-correlated single photon counting (TCSPC) method. Figure 6 shows the decay curves of monomer emission for the OPEN proteins (396 nm). The fluorescence decay for the CLOSED proteins was investigated at two wavelengths in the excimer emission region (450 and 485 nm), because the excimer emission caused by partially overlapping pyrene complexes appears at shorter wavelength regions with a smaller lifetime than that produced by a sandwich-type pyrene complex with sufficient ring overlap.[18] The investigation of fluorescence decay at the two wavelengths is essential to the assignment of multiphase fluorescence decay curves. The fluorescence decay curves at 450 and 485 nm for the CLOSED proteins are shown in Figure 7. Tables 3 and 4 list the monomer emission lifetimes for OPEN-form proteins and the excimer emission lifetimes for CLOSED-form proteins, respectively (the detailed kinetic analysis is shown in Figures S6, Supporting Information). The kinetic data for the CLOSED-form proteins in the presence of Mg^{2+} are also shown in Table S2 and Figure S7 (Supporting Information).

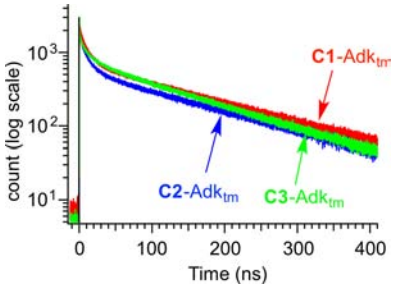

Figure 6. Fluorescence decay (396 nm) for the OPEN-form pyrene-labeled Adk$_{tm}$s (1 μM) in 50 mM Tris buffer (pH = 7.5) at 25 °C. A protein sample was irradiated at λ_{ex} = 375 nm with a pulse of fwhm = 64 ps.

Table 3. Lifetimes of Monomer Emission (396 nm) for the OPEN-Form Pyrene-Labeled Adk$_{tm}$s, Normalized Pre-Exponential Factors and χ^2 Values in the Curve-Fitting Analysis[a]

protein	$\tau_{1(OPEN)}$ (ns)	$\tau_{2(OPEN)}$ (ns)	χ^{2b}
C1-Adk$_{tm}$	9.93 (0.67)	163 (0.33)	1.04
C2-Adk$_{tm}$	10.0 (0.67)	159 (0.33)	1.02
C3-Adk$_{tm}$	9.83 (0.55)	140 (0.45)	1.10

[a]50 mM Tris buffer, pH 7.5, at 25 °C under a N_2 atmosphere, [protein] = 1 μM, λ_{ex} = 375 nm. The fluorescence lifetimes indicated in the table were based on the averages of three-run measurements. The values in parentheses indicate the normalized pre-exponential factors of each kinetic term. The uncertainties of fluorescence lifetimes are within 10%. [b]χ^2 value.

The monomer emission decay curves at 396 nm for the OPEN-form proteins were successfully analyzed using the double-exponential kinetic law. The lifetime of the fast phase, $\tau_{1(OPEN)}$, is almost identical among the three Adk$_{tm}$s (~10 ns). The lifetime $\tau_{2(OPEN)}$ is on the order of 10^2 ns. The double-exponential kinetic behavior and the order of lifetimes are similar to those previously reported for pyrene-labeled proteins[38] and molecular beacons.[3]

The fluorescence decay at 485 nm in the CLOSED **C1**-Adk$_{tm}$ required a curve-fitting analysis by the triple-exponential kinetic law, since a double-exponential kinetic analysis showed a

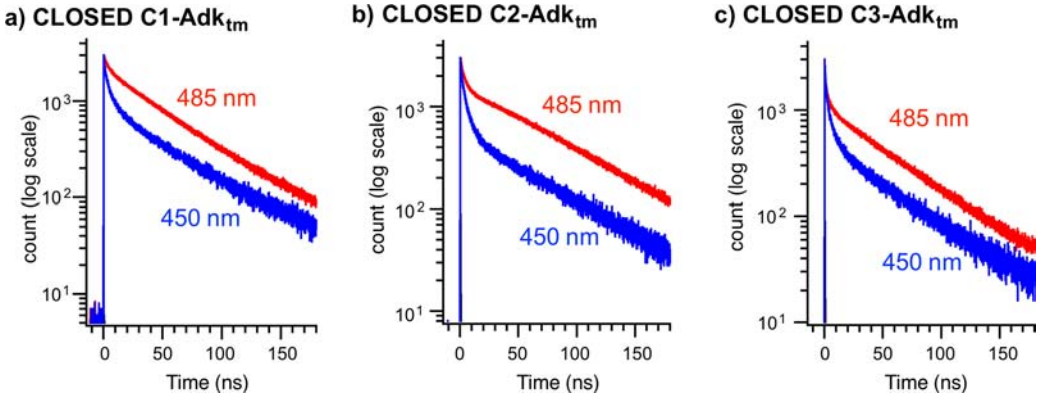

Figure 7. Fluorescence decay for CLOSED-form pyrene-labeled Adk$_{tm}$s (1 μM) at 450 nm (blue lines) and at 485 nm (red lines) in 50 mM Tris buffer (pH = 7.5) at 25 °C: (a) **C1**-Adk$_{tm}$; (b) **C2**-Adk$_{tm}$; (c) **C3**-Adk$_{tm}$. A protein sample was irradiated at λ_{ex} = 375 nm with a pulse of fwhm = 64 ps.

DOI: 10.1021/acs.bioconjchem.5b00026
Bioconjugate Chem. 2015, 26, 537−548

Table 4. Lifetimes of Excimer Emission (450 and 485 nm) for the CLOSED-Form Pyrene-Labeled Adk$_{tm}$s, Normalized Pre-Exponential Factors, and χ^2 Values in the Curve-Fitting Analysis[a]

protein	wavelength (nm)	$\tau_{1(CLOSED)}$ (ns)	$\tau_{2(CLOSED)}$ (ns)	$\tau_{2'(CLOSED)}$ (ns)	χ^{2b}
C1-Adk$_{tm}$[c]	485	3.41 (0.27)	40.4[d] (0.53)	81.3[d] (0.19)	0.92
	450	3.60 (0.62)	36.5[d] (0.26)	92.0[d] (0.12)	0.88
C2-Adk$_{tm}$[e]	485	2.69 (0.50)	69.0 (0.50)	------	0.92
	450	4.36[f] (0.80)	66.4 (0.20)	------	0.80
C3-Adk$_{tm}$[e]	485	2.35 (0.60)	58.2 (0.40)	------	1.01
	450	3.85 (0.79)	59.5 (0.21)	------	1.02

[a]50 mM Tris buffer, pH 7.5 at 25 °C under a N_2 atmosphere, [protein] = 1 μM and [Ap_5A] = 50 μM, λ_{ex} = 375 nm. The fluorescence lifetimes indicated in the table were based on the averages of three-run measurements. The values in parentheses indicate the fractions of each kinetic term. The uncertainties of fluorescence lifetimes are within 10% unless other noted. [b]χ^2 value. [c]Triple-exponential kinetic analysis was required to obtain a good χ^2 value. [d]Although the values of $\tau_{2(CLOSED)}$ and $\tau_{2'(CLOSED)}$ are similar, the separation into two kinetic terms for the later phase was required in curve-fitting analysis; otherwise, χ^2 value becomes more deviated from unity. Experimental scatters in lifetime values among three-run measurements are within 10%. These values are indicated as apparent lifetimes: The ratio of pre-exponential factors for these lifetimes does not reflect the real population ratio of each stacking mode, because the equilibrium constant between these stacking modes is not determined. [e]Double-exponential kinetic analysis was required to obtain a good χ^2 value. [f]The uncertainty may be larger than 10% because of χ^2 value significantly deviated from unity.

significant deviation at the initial stage of the fluorescence decay with a χ^2 value of >1.2. (see Figures S6−1 and S6−10, Supporting Information). The emission lifetime at the early stage ($\tau_{1(CLOSED)}$) was ∼3 ns, and the later phase in the fluorescence decay was featured by two lifetime parameters, $\tau_{2(CLOSED)}$ ∼ 40 ns and $\tau_{2'(CLOSED)}$ ∼ 80 ns. The fluorescence at 450 nm also decayed with similar lifetime values to those at 485 nm, although the pre-exponential factor of $\tau_{1(CLOSED)}$ at 450 nm was larger than that at 485 nm. Consequently, the initial decay of the excimer emission band ($\tau_{1(CLOSED)}$ ∼ 3 ns) is mainly caused by a component with fluorescence in the shorter wavelength region. In other words, the initial and later phases are assigned as the emissions from partially overlapping pyrene dimers and sandwich-like dimers, respectively (see the details in Discussion).[18,33] In contrast to the fluorescence decay in **C1**-Adk$_{tm}$, the fluorescence decay curves in the CLOSED **C2**- and **C3**-Adk$_{tm}$s were successfully analyzed using the double-exponential kinetic law. The lifetimes in the initial and later phases were similar to those of the CLOSED **C1**-Adk$_{tm}$ ($\tau_{1(CLOSED)}$ ∼ 3 ns and $\tau_{2(CLOSED)}$ = 55−70 ns). The pre-exponential factors of $\tau_{1(CLOSED)}$ in these proteins were found to be larger than that observed in the CLSOED **C1**-Adk$_{tm}$, indicating that partially overlapping pyrene dimers are predominant in the excited state for the CLOSED **C2**- and **C3**-Adk$_{tm}$s.

Although the steady-state fluorescence spectrum of the CLOSED **C1**-Adk$_{tm}$ showed a higher intensity of excimer emission in the presence of Mg^{2+} than that in the absence of Mg^{2+} (Figure 3A), no significant differences in the kinetic profile of fluorescence decay curves (lifetime and pre-exponential factors of each phase) were observed (Figure S7, Supporting Information). A similar trend was also seen in the CLOSED **C2**- and **C3**-Adk$_{tm}$s.

DISCUSSION

Effect of Nucleotide Structures on Steady-State Fluorescence Spectra. All pyrene-labeled Adk$_{tm}$s prepared in this work show the excimer emission around 485 nm upon the addition of Ap_5A in steady-state fluorescence spectra (Figure 3). The fluorescence spectral changes on the addition of nucleotide substrate molecules (ADP, ATP, or AMP) are similar among these proteins (Figure S3, Supporting Information). ADP produces the strongest excimer emission among nucleotide substrates. This fact indicates that the spectral changes caused by the nucleotide substrates surely reflect the substrate-binding fashion of Adk and the intrinsic characters of the structural transition of Adk: ADP occupies both ligand-binding sites (LID and NMP) to induce a *full* conformational change in Adk$_{tm}$, whereas ATP and AMP bring about a *partial* conformational change in the protein as they occupy only one of the binding sites.[30] This mechanism is schematically depicted in Figure S8 (Supporting Information).

Effect of Magnesium Ion on Steady-State Fluorescence Spectra. In **C1**-Adk$_{tm}$, the presence of Mg^{2+} brought out the further increase in the excimer emission intensity (and the concurrent decrease in the monomer emission), indicating that the binding of a magnesium ion to Adk causes the further conformational change in the CLOSED protein to affect the pyrene−pyrene stacking behavior. A magnesium ion is believed to interact with Asp84 and two oxygen atoms of the phosphate groups in ADP or ATP. It is supposed that the interaction contributes to the activation of the terminal phosphoryl group of a phosphate-donating substrate at the transition state[29,30,34] (see a schematic binding structure in Figure S9, Supporting Information). Thus, the protein-Ap_5A-Mg^{2+} ternary complex is a more analogous structure to the transition state in the phosphoryl transfer between two nucleotide substrates. In contrast to the CLOSED **C1**-Adk$_{tm}$, little effect of Mg^{2+} was observed on the emission spectra in the CLOSED **C2**- or **C3**-Adk$_{tm}$s (and I_R values). This is due to the increase in the degrees of freedom in the long linker moieties of probes **C2** and **C3**. On the basis of these findings, we can conclude that **C1** is the best probe for the sensitive detection of the microscopic structural change in Adk during the phosphoryl transfer between two substrate molecules.

Fluorescence Decay of Monomer Emission in the OPEN Adk$_{tm}$s. All the OPEN-form Adk$_{tm}$s showed the double-exponential fluorescence decay. The existence of a long lifetime fluorescence component ($\tau_{2(OPEN)}$ > 100 ns) popularly observed for pyrene in solutions[39] indicates that each pyrene is sufficiently isolated without protein−protein interactions. The origin of a short phase in the fluorescence decay is attributed to some weak interactions between a pyrene ring and peptide backbones (C−H···π interactions etc.) on the protein surface.[38,40] Another possible origin of the short phase is the light scattering effect in buffer solutions. This factor was proposed in research using a molecular beacon with pyrene moieties at the terminals of long alkyl chains, where few functional groups interacted with a π-conjugated ring existing

DOI: 10.1021/acs.bioconjchem.5b00026
Bioconjugate Chem. 2015, 26, 537−548

near the pyrene moieties.[3] Consequently, the observed short phase of the monomer emission decay in the OPEN-form Adk_{tm}s mainly originates from the interactions with peptide backbones and pyrene ring on the surface of Adk_{tm}.

Pyrene−pyrene Stacking Mode on the Surface of the CLOSED C1-Adk_{tm}. Among the pyrene-labeled Adk_{tm}s, **C1**-Adk_{tm} produces the strongest excimer emission, indicating that two pyrene rings of **C1**-Adk_{tm} are effectively arranged in proximity at the protein surface upon the binding of nucleotide ligands. According to the following spectroscopic characteristics in the CLOSED **C1**-Adk_{tm} ((i) broadened UV−vis and excitation spectra and (ii) the appearance of distinct exciton coupling-type signal in the CD spectrum), the excimer emission of the CLOSED **C1**-Adk_{tm} is denoted as "static excimer", where the two pyrene rings almost associate in the ground state.[18] The formation of a sandwich-like pyrene−pyrene stacking in the ground state is successfully shown in the X-ray single crystal structure of the CLOSED **C1**-Adk_{tm}.

However, the decay of excimer emission with multi-exponential kinetic behavior suggests the existence of several stacking modes between the two pyrenes at the excited state in solution. The appearance of a fast phase (lifetime $\tau_{1(CLOSED)}$) is ascribed to the existence of partially overlapping pyrene dimers. The assiginment is based on the large pre-exponential factor of the initial emission decay (~3 ns) at 450 nm (in the shorter-wavelength skirt of the excimer emission band). However, sandwich-like pyrene stacking is predominant in the CLOSED **C1**-Adk_{tm}, although partially overlapping pyrene complexes also exist to a certain extent in solution. Interactions between the pyrene ring and peptide backbones may contribute to the initial emission decay, as considered for the fluorescence decay traces of OPEN-form proteins. However, the factor derived from the $\pi-\pi$ stacking of pyrenes is more significant. This is supported by the experimental finding that the pre-exponential factor of lifetime $\tau_{1(CLOSED)}$ is dependent on measurement wavelength. Furthermore, the observation of two lifetime parameters for the slower phase on the emission decay of the CLOSED **C1**-Adk_{tm} suggests that at least two different orientations of pyrene dimers exist among the sandwich-like dimers at the excited state. A similar kinetic behavior was also reported in a pyrene-conjugated dendrimer,[20] pyrenes at the interface of polymer Langmuir−Blodgett films,[23] and pyrene-end-capped polymers.[25] In these reports, several pyrene orientations and the equilibrium between twisted stacking and parallel stacking of pyrenes were proposed to exist.

Although the steady-state fluorescence and CD spectra for the CLOSED **C1**-Adk_{tm} are influenced by the presence of Mg^{2+}, the kinetic profiles of the fluorescence decay are largely unaffected by the presence of Mg^{2+} (Figure S7, Supporting Information). A possible reason for the discrepancy between the profiles in the steady-state and time-resolved measurements is attributed to a rapid equilibrium between pyrene stacking modes (on the nanosecond scale) during the transition from the excited state to the ground state, regardless of the presence or absence of Mg^{2+}.[41]

Pyrene−pyrene Stacking Mode on the Surface of the CLOSED C2- and C3-Adk_{tm}s. The pre-exponential factor of $\tau_{1(CLOSED)}$ at 485 nm is ranked as **C1**-Adk_{tm} ≪ **C2**-Adk_{tm} < **C3**-Adk_{tm}. This is due to an increase in the contribution of the emission caused by partially overlapping dimers in the **C2**- and **C3**-Adk_{tm} because of the increase in the linker length. Consequently, the population of partially overlapping pyrene dimer is predominant in the CLOSED **C2**- and **C3**-Adk_{tm} in the excited state. The later phase of the emission decay originates from sandwich-like pyrene dimers, although the contribution of the stacking modes to excimer emission is small in these proteins. A remarkable fact is that no separation into two phases occurs at the later emission decay phase in these proteins. This is because pyrene dimers with sufficient ring overlap but several orientations (e.g., twisted association) in the excited states are in rapid equilibrium, resulting in the exhibition of apparently averaged fluorescence decay.

In the CLOSED **C2**- and **C3**-Adk_{tm}s, the broadening in the UV−vis and excitation spectra in the excimer is smaller than those of the CLOSED **C1**-Adk_{tm}. This spectral characteristic implies that the association of pyrene rings in the ground state is weak. When pyrene rings are within a distance that is sufficient to form a stacked conformation, the occurrence of "dynamic excimer" is expected. Dynamic excimer of pyrene is, normally, characterized by an initial growth followed by a decay in fluorescence around 485 nm after excitation.[18] However, the rise in fluorescence during the initial phase was not experimentally observed in this work. A possible reason for the fluorescence change is the very fast formation of a dynamic excimer within the pulse irradiation time (64 ps),[42] because of the preset proximity of two cysteine residues anchoring the pyrene moieties (ca. 12 Å).

Although no direct experimental evidence indicating the formation of a dynamic excimer is available at present, the following spectroscopic characteristics suggest that the conformational fluctuation in pyrene−pyrene stacking at the excited state significantly contributes to the excimer emission properties of the CLOSED **C2**-Adk_{tm}: (i) The smallest ΔP_{abs} and ΔP_{excit} values among the Adk_{tm}s imply weak association in the ground state. (ii) The largest decrease in the value of Φ_F upon the addition of Ap_5A (−0.12 in **C1**-Adk_{tm}, −0.16 in **C2**-Adk_{tm}, and −0.08 in **C3**-Adk_{tm}) suggests enhancement of nonradiative processes because of the increased flexibility in the linker moiety. (iii) In spite of the aforementioned spectroscopic characteristics, as shown in Supporting Information Figure S10, the ratio of fluorescence intensities at 450 nm (in the short-wavelength skirt of the excimer emission band; dominated by partial stacking) and 520 nm (in the long-wavelength skirt of the excimer emission band; dominated by sandwich-like stacking) in the CLOSED **C2**-Adk_{tm} is almost the same as that in the CLOSED C1-Adk_{tm} and is larger than that in the CLOSED C3-Adk_{tm} (I_{520}/I_{450} = 1.49, 1.50, and 1.26 for **C1**-, **C2**-, and **C3**-Adk_{tm}, respectively). The finding described in the section (iii) indicates that the excimer emission for the CLOSED **C2**-Adk_{tm} observed by steady-state fluorescence spectroscopy is predominated by a similar population of sandwich-type dimers to that in the CLOSED **C1**-Adk_{tm}, although the fluorescence decay profiles in the time-resolved fluorescence measurements are quite different between the two proteins. These spectroscopic features shown in the steady-state and time-resolved measurements highlight the utility of the combination of these spectroscopic techniques for precise understanding of the interaction modes between two chromophore probes with flexible linkers that are attached to a biomolecule.

Significance of the Probe Structure Optimization. Among the three pyrene-labeled Adk_{tm}s, the fluorescence changes in **C1**-Adk_{tm} most faithfully reflect the intrinsic structural change in Adk (i.e., OPEN/CLOSED transition and the conformational effect at the transition state by a magnesium ion). Probe **C1** thus can be considered as the best

DOI: 10.1021/acs.bioconjchem.5b00026
Bioconjugate Chem. 2015, 26, 537−548

candidate for evaluating the conformational fluctuation of a protein.

We can expect that the interactions between two pyrene rings are inhibited with the increase in the linker flexibility of pyrene probes. However, in reality, the relationship between the spectral characteristics and the length of a linker is not straightforward. The values of ΔP_{abs} and ΔP_{excit} of **C3**-Adk$_{tm}$ are slightly higher than those of **C2**-Adk$_{tm}$ (see Table 2), indicating that the association of pyrene in the CLOSED **C3**-Adk$_{tm}$ at the ground state occurs more easily than the CLOSED **C2**-Adk$_{tm}$ in spite of the more flexible and longer linker in **C3**. Nevertheless, the ratio of fluorescence intensities at 520 nm and 450 nm (I_{520}/I_{450}) indicates that the excimer emission of the CLOSED **C3**-Adk$_{tm}$ is more predominantly caused by the partially overlapping pyrenes, compared to the CLOSED **C2**-Adk$_{tm}$. In other words, the pyrene−pyrene interaction in the CLOSED **C3**-Adk$_{tm}$ weakens at the excited state. A probe molecule with an excessively long linker moiety sometimes presents challenges in the interpretation of spectroscopic characteristics. Thus, the optimization of a chromophore probe structure is critical when the probe is introduced into a flexible part of the target biomolecule for evaluating the conformational effect around the part.

CONCLUSION

Fluorescence properties of the A55C/C77S/V169C adenylate kinase mutants modified by three kinds of pyrenyl iodoacetamide were investigated in terms of pyrene stacking modes on the protein surface. Regardless of the lengths in the linker moiety, all the proteins are able to form the CLOSED form with a similar distance between Cys55 and Cys169. However, the mechanism of excimer emission in the CLOSED Adk$_{tm}$s is strongly dependent on the linker length of the pyrene probes. The excimer emission of the CLOSED pyrene-labeled Adk$_{tm}$ with a short methylene linker is almost predominated by "static excimer" of pyrene dimers with sufficient ring overlap. The stacking mode is clearly shown in the X-ray crystallographic analysis for the CLOSED **C1**-Adk$_{tm}$. In contrast, the stacking fluctuation at ground and/or excited states becomes significant with the increase in the linker length, which is shown in less broadening in the UV−vis/excitation spectra and fluorescence decay profiles of **C2**- and **C3**-Adk$_{tm}$s. The difference in only one carbon unit of methylene linkage is able to produce a dramatic difference in the fluorescence decay profiles. These fluorescence properties indicate the need for optimization of the structure of a pyrene probe for correctly evaluating spatial information between pyrene-labeled places in a biomolecule or between pyrene-labeled biomolecules. This matter will be more critical when the flexibilities of synthetic probes and/or conjugation sites in targeted biomolecules increase. In this context, a series of spectroscopic data presented in this work demonstrate (i) the significance of probe structure design and (ii) the utility of the combination of steady-state and time-resolved spectroscopic measurements for the precise evaluation of the association modes between fluorescent probe-labeled biomolecules (distance, orientation, fluctuation of interaction modes in the ground and excited states).

EXPERIMENTAL SECTION

Materials and Instruments. All chemicals were obtained from conventional commercial sources and used as received unless otherwise noted. The synthesis of pyrenyl iodoacetamide **C1** was described in a previous report.[26] The syntheses of pyrenyl iodoacetamides **C2** and **C3** are described above (see the detailed synthetic procedures in Supporting Information). The plasmid pEAK91 harboring Adk$_{tm}$ (A55C/C77S/V169C) was prepared from the plasmid coding the double mutant of *E. coli*. Adk (A55C/C77S) (gifted by Prof. E. Haas, Bar-Ilan Univ., Israel) according to our previous report.[26] Hexokinase and gluclose-6-phosphate dehydrogenase from baker's yeast were purchased from Sigma as a mixed material (catalog code: H8629−500UN).

NMR spectra were collected on a JEOL JNM-ECP400 spectrometer. The ^{1}H NMR and ^{13}C NMR chemical shifts are reported in ppm relative to tetramethylsilane (TMS) or the residual solvent protons. Protein purification was conducted using a ÄKTA FPLC chromatography system in a chromatochamber (4 °C). ESI-MS analyses were carried out using a JEOL JMS-T100LC mass spectrometer. MALDI-TOF-MS analyses were conducted using a Bruker Autoflex II mass spectrometer. UV−vis spectra were measured using a Shimadzu UV-2550 double beam spectrophotometer. CD (circular dichroism) spectra were collected using a JASCO J-725 circular dichroism spectrophotopolarimeter. Steady-state fluorescence spectra were measured using a JASCO FP-8300 fluorescence spectrophotometer equipped a with thermostated cell holder. Fluorescence lifetimes were measured by the time-correlated single photon counting (TCSPC) method using a FluoTime 200 (PicoQuant) TCSPC spectrophotometer with a picosecond laser system (LDH-P-C-375 and PDL-200B, PicoQuant).

Expression and Purification of Adk$_{tm}$. The Adk$_{tm}$ expression system was constructed by the transformation of *E. coli* HB101 using the pEAK91 plasmid harboring Adk$_{tm}$. Protein expression and purification were carried out in the same manner as the method described in a previous report.[26] Protein samples were stored in 40 mM sodium phosphate buffer (pH = 6.5) containing 50%(v/v) glycerol, 100 mM NaCl, 2 mM ethylenediamine-*N,N,N′,N′*-tetraacetic acid disodium salt (EDTA), and 2 mM dithiothreitol (DTT) at −20 °C.

Conjugation of Pyrenyl Iodoacetamides (C1, C2, or C3) to Adk$_{tm}$. A protein solution was passed through a PD-10 column (GE healthcare) with elution of 50 mM HEPES (pH = 8.0) to remove glycerol and DTT, immediately before use. A pyrenyl iodoacetamide (50 equiv) dissolved in DMSO was added to the buffer solution of protein (2 μM) with adjustment of the concentration of DMSO to 5% (v/v) in final solution. The mixed solution was gently stirred at 25 °C for 24 h in the dark. After the solution was centrifuged, the supernatant was dialyzed against 20 mM Tris buffer (pH = 8.0). The protein solution was subjected to a MonoQ anionic exchange column (5 mL, GE healthcare) to separate from the unmodified and partially modified proteins (flow rate: 0.5 mL/min, eluent: 20 mM Tris buffer (pH = 8.0) with linear gradient of NaCl from 0 to 300 mM). The pyrene-labeled protein was eluted at the elution volume of 26−30 mL (for **C1**-Adk$_{tm}$), 31−34 mL (for **C2**-Adk$_{tm}$), and 32−35 mL for (**C3**-Adk$_{tm}$). The chromatograms in the protein purification are shown in Figure S11 (Supporting Information). The collected protein solution was desalted using a HiTrap desalting column (5 mL, GE healthcare), lyophilized, and kept at −80 °C. The introduction of two pyrene moieties into Adk$_{tm}$ was confirmed by MALDI-TOF-MS analyses (Figure S12 in Supporting Information).

DOI: 10.1021/acs.bioconjchem.5b00026
Bioconjugate Chem. 2015, 26, 537−548

Confirmation of Adk Activities of Adk$_{tm}$s. The phosphoryl transfer activities of Adk$_{tm}$s were measured by monitoring the formation of NADPH (the increase in absorbance at 340 nm) produced by the Adk$_{tm}$-hexokinase-glucose-6-phosphate dehydrogenase tandem reaction[32] in 50 mM Tris buffer (pH = 7.5) at 25 °C. The measurement conditions were as follows: [Adk$_{tm}$] = 44 nM, [ADP] = 2 mM, [glucose] = 10 mM, [NADP$^+$] = 2.3 mM, and hexokinase/glucose-6-phosphate dehydrogenase = 25 unit.

Measurements of UV−vis, Steady-State Fluorescence, and CD Spectra. All UV−vis, steady-state fluorescence, and CD spectra were collected in a 1 cm quartz cell at 25 °C. The wavelength resolution in UV−vis spectra was 0.5 nm. CD spectra were obtained by accumulation of five scans with 1 nm-resolution. Steady-state fluorescence spectra were collected at the excitation wavelength of 345 nm and recorded at 1 nm resolution.

Measurements of Fluorescence Quantum Yields. The relative fluorescence quantum yields of a pyrene-labeled Adk$_{tm}$ (Φ_Fs) were determined using the quantum yield of 9,10-diphenylanthtracene (Φ_{st} = 0.95) in ethanol as a reference.[43] The Φ_F was calculated with the following equation (eq 1):[3]

$$\phi_F = \phi_{st} \frac{\int I_P}{\int I_{st}} \frac{A_{st}}{A_P} \frac{Ri_W{}^2}{Ri_E{}^2} \quad (1)$$

where $\int I_P$ is the integrated fluorescence intensity of a pyrene-labeled Adk$_{tm}$, $\int I_{st}$ is the integrated fluorescence intensity of the standard sample, and A_{st} and A_P is the absorbance of the standard sample and the protein samples at the excitation wavelength (340 nm), respectively. Ri_W and Ri_E are refractive indexes of water and ethanol, respectively (Ri_W = 1.333 and Ri_E = 1.362).

Measurements of Fluorescence Lifetimes. Samples for TCSPC fluorescence lifetime measurements were anaerobically prepared and sealed with a septum to avoid air contact. After the sample solution was excited at 375 nm by a laser pulse with full width at a half-maximum (fwhm) of 64 ps, the fluorescence decays at 396 nm (for OPEN-form proteins) and 450 and 485 nm (for CLOSED-form proteins) were monitored at 25 °C with a time resolution of 64 ps. The excitation wavelength was selected in order to avoid the complexity caused by the excitation of pyrene to higher energy levels than S_1-state. The fluorescence decay obtained was analyzed by (eq 2):

$$I(t) = \int_{-\infty}^{t} F_{IR}(t') \sum_{i=1}^{n} A_i \exp\left(-\frac{t-t'}{\tau_i}\right) dt' \quad (2)$$

where $I(t)$ is the observed fluorescence decay, $F_{IR}(t')$ is the instrument response function of excitation pulse, A_i is a fraction of decay component i, and τ_i is a fluorescence relaxation time (lifetime) of decay component i.

Crystallization and X-ray Diffraction Collection of the CLOSED C1-Adk$_{tm}$. To a concentrated solution of purified **C1**-Adk$_{tm}$ sample in 50 mM Tris buffer (pH = 7.5, 8.5 mg/mL) was added $MgCl_2$ and Ap_5A in water (2 mM in final). The **C1**-Adk$_{tm}$ crystals used for X-ray diffraction were prepared by hanging-drop vapor-diffusion method at 20 °C. The crystals were grown in 0.2 μL solutions that contained 0.1 μL of **C1**-Adk$_{tm}$ solution and 0.1 μL of reservoir solution (0.1 M HEPES sodium pH = 7.5, and 0.8 M potassium sodium tartrate tetrahydrate), equilibrated against 50 μL of the reservoir solution. Crystals were each mounted into a loop and then flash-frozen in a stream of N_2 at 100 K. Diffraction data were collected at 100 K synchrotron radiation at the SPring-8 BL32XU (Japan). The diffraction data sets were processed using HKL2000.[44]

Structure Determination and Refinement of CLOSE C1-Adk$_{tm}$ Crystal. The crystal structure of the CLOSED **C1**-Adk$_{tm}$ was solved by molecular replacement with the program Molrep, using the wild-type Adk in complex with Ap_5A (PDB ID: 1AKE) as a search model. Model refinement was using CNS,[45] with manual inspection and modification in conjunction with the CCP4 program COOT.[46] NCS averaging between two monomers within the dimer was attempted but did not improve the calculated electron density maps; thus, no NCS restraints were applied. The $\varphi-\phi$ angles of >90% of the residues in the C1-Adk$_{tm}$ structure are in the most favored regions of the Ramachandran plot as assessed by Molprobity.[47] Phasing and refinement statistics are given in Supporting Information Table S1. Figures were prepared using Pymol (www.pymol.org). The final atomic coordinates and structure-factor amplitudes of **C1**-Adk$_{tm}$ (PDB ID: 3X2S) were deposited in the Worldwide Protein Data Bank (wwPDB; http://www.wwpdb.org) and the Protein Data Bank Japan at the Institute for Protein Research, Osaka University, Suita, Osaka, Japan (PDBj; http://www.pdbj.org/).

■ ASSOCIATED CONTENT

Supporting Information

Data from X-ray crystallographic analysis, lifetimes obtained in the presence of Mg^{2+}, CD spectra for Adk$_{tm}$s, Adk activity assays, fluorescence spectral changes on the addition of substrate ligands, excitation spectra of Adk$_{tm}$s, kinetic analyses of lifetime measurements, schematically depicted relationship between substrate-binding fashion and excimer emission, overlaid excimer emission spectra (normalized) of Adk$_{tm}$s, chromatograms in protein purification and MALDI-TOS-MS spectra of Adk$_{tm}$s. This material is available free of charge via the Internet at http://pubs.acs.org.

■ AUTHOR INFORMATION

Corresponding Authors

*E-mail: matsumura@chem.eng.osaka-u.ac.jp (H. M.).
*E-mail: wschung@nctu.edu.tw (W.-S. C.).
*E-mail: tmatsuo@ms.naist.jp (T. M.).

Notes

The authors declare no competing financial interest.

■ ACKNOWLEDGMENTS

The authors thank financial support from a Grant-in-Aid for Science Research on Innovative Areas ("Stimuli-responsive Chemical Species for the Creation of Functional Molecules", MEXT, Japan), Innovations Inspired by Nature Research Program by Sekisui Integrated Research, Inc., and "The Green Photonics Project" (NAIST, Japan). This work was supported by the Platform for drug discovery, informatics, and structural life science (MEXT, Japan). The authors acknowledge Prof. Eric Wei-Guang Diau, Dr. Hung-Yu Hsu, and Ms. Yu-Pei Huang (National Chiao Tung University, Taiwan) for helping us with the TCSPC measurements.

DOI: 10.1021/acs.bioconjchem.5b00026
Bioconjugate Chem. 2015, 26, 537−548

REFERENCES

(1) Bains, G., Patel, A. B., and Narayanaswami, V. (2011) Pyrene: A probe to study protein conformation and conformational changes. *Molecules 16*, 7909−7935.

(2) Bains, G. K., Kim, S. H., Sorin, E. J., and Narayanaswami, V. (2012) The extent of pyrene excimer fluorescence emission is a reflector of distance and flexibility: analysis of the segment linking the LDL receptor-binding and tetramerization domains of apolipoprotein E3. *Biochemistry 51*, 6207−6219.

(3) Conlon, P., Yang, C. -Y. J., Wu, Y.-R., Chen, Y., Martinez, K., Kim, Y.-M., Stevens, N., Marti, A. A., Jockusch, S., Turro, N. J., et al. (2008) Pyrene excimer signaling molecular beacons for probing nucleic acids. *J. Am. Chem. Soc. 130*, 336−342.

(4) Nakamura, M., Fukuda, M., Takada, T., and Yamana, K. (2012) Highly ordered pyrene π-stacks on an RNA duplex display static excimer fluorescence. *Org. Biomol. Chem. 10*, 9620−9626.

(5) Karlsen, K. K., Okholm, A., Kjems, J., and Wengel, J. (2013) A quencher-free molecular beacon design based on pyrene excimer fluorescence using pyrene-labeled UNA (unlocked nucleic acid). *Bioorg. Med. Chem. 21*, 6186−6190.

(6) Fujimoto, K., Yamada, S., and Inouye, M. (2009) Synthesis of versatile fluorescent sensors based on Click chemistry: detection of unsaturated fatty acids by their pyrene-emission switching. *Chem. Commun.*, 7164−7166.

(7) Qing, Z. H., He, X. X., Huang, J., Wang, K. M., Zou, Z., Qing, T. P., Mao, Z. G., Shi, H., and He, D. G. (2014) Target-catalyzed synamic assembly-based pyrene excimer switching for enzyme-free nucleic acid amplified detection. *Anal. Chem. 86*, 4934−4939.

(8) You, L., and Gokel, G. W. (2008) Fluorescent, synthetic amphiphilic heptapeptide anion transporters: Evidence for self-assembly and membrane localization in liposomes. *Chem.—Eur. J. 14*, 5861−5870.

(9) Frañová, M. D., Vattulainen, I., and Ollila, O. H. S. (2014) Can pyrene probes be used to measure lateral pressure profiles of lipid membranes? Perspective through atomistic simulations. *Biochim. Biophys. Acta 1838*, 1406−1411.

(10) Förster, T. (1969) Excimers. *Angew. Chem., Int. Ed. in Engl. 8*, 333−343.

(11) Kano, K., Matsumoto, H., Hashimoto, S., Sisido, M., and Imanishi, Y. (1985) Chiral pyrene excimer in the γ-cyclodextrin cavity. *J. Am. Chem. Soc. 107*, 6117−6118.

(12) Ueno, A., Suzuki, I., and Osa, T. (1989) Association dimers, excimers, and inclusion complexes of pyrene-appended γ-cyclodextrins. *J. Am. Chem. Soc. 111*, 6391−6397.

(13) Sinev, M. A., Sineva, E. V., Ittah, V., and Haas, E. (1996) Domain closure in adenylate kinase. *Biochemistry 35*, 6425−6437.

(14) Chen, S. X., Wang, L., Fahmi, N. E., Benkovic, S. J., and Hecht, S. M. (2012) Two pyrenylalanines in dihydrofolate reductase form an excimer enabling the study of protein dynamics. *J. Am. Chem. Soc. 134*, 18883−18885.

(15) Maeda, H., Maeda, T., Mizuno, K., Fujimoto, K., Shimizu, H., and Inouye, M. (2006) Alkynylpyrenes as improved pyrene-based biomolecular probes with the advantages of high fluorescence quantum yields and long absorption/emission wavelengths. *Chem.—Eur. J. 12*, 824−831.

(16) Senthilvelan, A., Ho, I.-T., Chang, K.-C., Lee, G.-H., Liu, Y.-H., and Chung, W.-S. (2009) Cooperative recognition of a copper cation and anion by a calix[4]arene substituted at the lower rim by a β-amino-α,β-unsaturated ketone. *Chem.—Eur. J. 15*, 6152−6160.

(17) Hung, H.-C., Chang, Y.-Y., Luo, L., Hung, C.-H., Diau, E. W.-G., and Chung, W.-S. (2014) Different sensing modes of fluoride and acetate based on a calix[4]arene with 25,27-bistriazolylmethylpyrenylacetamides. *Photochem. Photobiol. Sci. 13*, 370−379.

(18) Winnik, F. M. (1993) Photophysics of preassociated pyrenes in aqueous polymer solutions and in other organized media. *Chem. Rev. 93*, 587−614.

(19) Birks, J. B. (1975) Excimers. *Rep. Prog. Phys. 38*, 903−974.

(20) Lekha, P. K., and Prasad, E. (2011) Tunable emission of static excimer in a pyrene-modified polyamidoamine dendrimer aggregate through positive solvatochromism. *Chem.—Eur. J. 17*, 8609−8617.

(21) Yamazaki, I., Winnik, F. M., Winnik, M. A., and Tazuke, S. (1987) Excimer formation in pyrene labeled hydroxypropyl cellulose in water. Picosecond fluorescence studies. *J. Phys. Chem. 91*, 4213−4216.

(22) Matsui, J., Mitsuishi, M., and Miyashita, T. (2002) Dynamic behavior of pyrene fluorescence in highly oriented polymer LB films. *Colloids Surf., A 198*, 703−707.

(23) Matsui, J., Mitsuishi, M., and Miyashita, T. (2002) A study on fluorescence behavior of pyrene at the interface of polymer Langmuir-Blodgett films. *J. Phys. Chem. B 106*, 2468−2473.

(24) de Melo, J. S., Costa, T., Miguel, M. D., Lindman, B., and Schillén, K. (2003) Time-resolved and steady-state fluorescence studies of hydrophobically modified water-soluble polymers. *J. Phys. Chem. B 107*, 12605−12621.

(25) Costa, T., de Melo, J. S., and Burrows, H. D. (2009) Fluorescence behavior of a pyrene-end-capped poly(ethylene oxide) in organic solvents and in dioxane-water mixtures. *J. Phys. Chem. B 113*, 618−626.

(26) Fujii, A., Hirota, S., and Matsuo, T. (2013) Reversible switching of fluorophore property based on intrinsic conformational transition of adenylate kinase during itscatalytic cycle. *Bioconjugate Chem. 24*, 1218−1225.

(27) Wieland, B., Tomasselli, A. G., Noda, L. H., Frank, R., and Schulz, G. E. (1984) The amino-acid-sequence of GTP−AMP phosphotransferase from beef-heart mitochondria. Extensive homology with cytosolic adenylate kinase. *Eur. J. Biochem. 143*, 331−339.

(28) Gerstein, M., Schulz, G., and Chothia, C. (1993) Domain closure in adenylate kinase - Joints on either side of 2 helices close like neighboring fingers. *J. Mol. Biol. 229*, 494−501.

(29) Müller, C. W., and Schulz, G. E. (1992) Structure of the complex between adenylate kinase from Escherichia coli and the inhibitor Ap_5A refined at 1.9 Å resolution. A model for a catalytic transition-state. *J. Mol. Biol. 224*, 159−177.

(30) Krishnamurthy, H., Lou, H. F., Kimple, A., Vieille, C., and Cukier, R. I. (2005) Associative mechanism for phosphoryl transfer: A molecular dynamics simulation of Escherichia coli adenylate kinase complexed with its substrates. *Proteins 58*, 88−100.

(31) Blanchette, M. A., Choy, W., Davis, J. T., Essenfeld, A. P., Masamune, S., Roush, W. R., and Sakai, T. (1984) Horner-Wadsworth-Emmons reaction. Use of lithium chloride and an amine for base sensitive compounds. *Tetrahedron Lett. 25*, 2183−2186.

(32) Kunst, A., Draeger, B., and Ziegenhorn, J. (1984) UV-methods with hexokinase and glucose-6-phosphate dehydrogenase. In *Methods of Enzymatic Analysis* (Bergmeyer, H. U., Ed.) pp 163−172, Verlag Chemie, Weinheim, Germany.

(33) No influence of the stacking between an adenine moiety in Ap_5A and a pyrene ring on the fluorescence spectrum of pyrene occurs at the measurement conditions (the 10 μM-order of Ap_5A). See also Figures 7 and S7 in ref 26.

(34) Tan, Y.-W., Hanson, J. A., and Yang, H. (2009) Direct Mg^{2+} binding activates adenylate kinase from Escherichia coli. *J. Biol. Chem. 284*, 3306−3313.

(35) Chakrabartty, A., Kortemme, T., Padmanabhan, S., and Baldwin, R. L. (1993) Aromatic side-chain contribution to far-ultraviolet circular-dichroism of helical peptides and its effect on measurement of helixpropensities. *Biochemistry 32*, 5560−5565.

(36) Zsila, F. (2003) A new ligand for an old lipocalin: induced circular dichroism spectra reveal binding of bilirubin to bovine beta-lactoglobulin. *FEBS Lett. 539*, 85−90.

(37) The CD signals caused by electronic/magnetic diople interacions between a π-ring system and an amide carbonyl group has been investigated using an amino acid-modified porphyrin. Mizutani, T., Ema, T., Yoshida, T., Renné, T., and Ogoshi, H. (1994) Mechanism of induced circular-dichroism of amino-acid ester-porphyrin supramolecular systems. Implications to the origin of the circular-dichroism of hemoprotein. *Inorg. Chem. 33*, 3558−3566.

DOI: 10.1021/acs.bioconjchem.5b00026
Bioconjugate Chem. 2015, 26, 537−548

(38) Weltman, J. K., Szaro, R. P., Frackelton, A. R., Jr., Dowben, R. M., Bunting, J. R., and Cahou, R. E. (1973) N-(3-Pyrene)maleimide: a long lifetime fluorescent sulfhydryl reagent. *J. Biol. Chem. 248*, 3173−3177.
(39) Birks, J. B., Dyson, D. J., and Munro, I. H. (1963) 'Excimer' fluorescence. II. Lifetime studies of pyrene solutions. *Proc. R. Soc. London, Ser. A 275*, 575−588.
(40) Preuss, R., Dapprich, J., and Walter, N. G. (1997) Probing RNA-protein interactions using pyrene-labeled oligodeoxynucleotides: Qβ replicase efficiently binds small RNAs by recognizing pyrimidine residues. *J. Mol. Biol. 273*, 600−613.
(41) The lifetime values $\tau_{2(\mathrm{CLOSED})}$ and $\tau_{2'(\mathrm{CLOSED})}$ listed in Tables 4 and S2 are apparent parameters determined by the decay curve-fitting analyses. The equilibrium constant between pyrene-stacking species was not considered in this work. Consequntly, detailed quantitative interpretation for the population of each pyrene staclking mode based on the ratio of pre-exponential factors is impossible.
(42) Although we attempted time-resolved up-conversion fluorescence measurements (fwhm = 0.27 ps), the intrinsic low sensitivity in the method prevented us to see a fluorescence rising phase clearly.
(43) Morris, J. V., Mahaney, M. A., and Huber, J. R. (1976) Fluorescence quantum yield determinations - 9,10-diphenylanthracene as a reference-standard in different solvents. *J. Phys. Chem. 80*, 969−974.
(44) Otwinowski, Z. (1993) Oscillation data reduction program. *Proceedings of the CCP4 Study Weekend on Data Collection and Processing* (Sawyer, L., Isaacs, N., and Bailey, S., Eds.) pp 56−62; Daresbury Laboratory; Warrington.
(45) Brunger, A. T., Adams, P. D., Clore, G. M., DeLano, W. L., Gros, P., Grosse-Kunstleve, R. W., Jiang, J. S., Kuszewski, J., Nilges, M., Pannu, N. S., et al. (1998) Crystallography & NMR system: A new software suite for macromolecular structure determination. *Acta Crystallogr., Sect. D 54*, 905−921.
(46) Emsley, P., and Cowtan, K. (2004) Coot: model-building tools for molecular graphics. *Acta Crystallogr., Sect. D 60*, 2126−2132.
(47) Davis, I. W., Leaver-Fay, A., Chen, V. B., Block, J. N., Kapral, G. J., Wang, X., Murray, L. W., Arendall, W. B., 3rd, Snoeyink, J., Richardson, J. S., and Richardson, D. C. (2007) MolProbity: all-atom contacts and structure validation for proteins and nucleic acids. *Nucleic Acids Res. 35*, 375−383.

DOI: 10.1021/acs.bioconjchem.5b00026
Bioconjugate Chem. 2015, 26, 537−548